

# Temperature-dependent collective effects for silicene, germanene and monolayer black phosphorus

Andrii Iurov\*

*Center for High Technology Materials, University of New Mexico,  
1313 Goddard SE, Albuquerque, NM, 87106, USA*

Godfrey Gumbs

*Department of Physics and Astronomy, Hunter College of the City University of New York,  
695 Park Avenue, New York, NY 10065, USA and  
Donostia International Physics Center (DIPC), P de Manuel Lardizabal,  
4, 20018 San Sebastian, Basque Country, Spain*

Danhong Huang

*Air Force Research Laboratory, Space Vehicles Directorate,  
Kirtland Air Force Base, NM 87117, USA and  
Center for High Technology Materials, University of New Mexico,  
1313 Goddard SE, Albuquerque, NM, 87106, USA*

(Dated: July 17, 2021)

We have calculated numerically electron exchange, correlation energies and dynamical polarization function for newly discovered silicene, germanene and black phosphorus (BP), consisting of puckered layers of elemental phosphorus atoms, broadening the range of two-dimensional (2D) materials at various temperatures. As a matter of fact, monolayer BP, produced by mechanical and liquid exfoliation techniques, has been predicted to be an insulator with a large energy splitting  $\approx 1.6$  eV for the quasiparticle band structure. We compare the dependence of these energies on the chemical potential, field-induced gap and the temperature and concluded that in many cases they behave qualitatively similarly, i.e., increasing with the doping, decreasing significantly at elevated temperatures, and displaying different dependence on the asymmetry gap at various temperatures. Furthermore, we used the dynamical polarizability to investigate the new “split” plasmon branches in the puckered lattices and predict a unique splitting, different from that in gapped graphene, for various energy gaps. Our results are crucial for stimulating electronic, transport and collective studies of these novel materials, as well as for enhancing silicene-based fabrication and technologies for photovoltaics and transistor devices.

arXiv:1605.08747v1 [cond-mat.mes-hall] 27 May 2016

---

\* aiurov@unm.edu

Since high-quality graphene crystal became available in 2004, its transport and optical properties due to quantum confinement have been extensively studied both theoretically and experimentally. In particular, free-standing graphene is a semiconductor but silicene, a buckled structure in which the silicon atoms are displaced perpendicular to the basal plane, as well as black phosphorus have been broadening interest in two-dimensional materials because of the presence of a larger gap between the quasiparticle energy bands. This gives rise to the possibility of novel practical applications. [1–3] It is well known that graphene exhibits a number of interesting properties which are related to its novel electronic structure near the Fermi level, represented by the so-called Dirac cone. Due to this unique linear dispersion and chirality, graphene electrons may not be confined by electrostatic gate voltage or energy barriers. Such a situation changes when there is a gap between the valence and conduction bands. Consequently, gap opening and its related tunability become a crucial issue for developing novel transistor technologies. This goal could be achieved by employing graphene nanoribbons, putting graphene on various insulating substrates [4–7] or even under illumination by circularly-polarized light. [8]

Flexibly-tuned phase transitions between insulating and conducting states were predicted theoretically and then demonstrated experimentally for puckered lattices of other fourth- and fifth-group elements, such as silicene, germanene and black phosphorus [9, 10]. In contrast to the carbon-based graphene, Si and Ge atoms have a larger ionic radius, making  $sp^3$  hybridization energetically favorable and leading to out-of-plane buckling and asymmetry between sublattices. Obviously, the bandgap induced by buckling could be tuned by applying an electric field perpendicular to the silicene plane. Such predicted bandgap tunability may be easily realized in experiments. [11–13]

Following the epitaxial growth of silicene in 2010, considerable attention has been devoted to understanding its microscopic electronic properties which have led to silicene being an excellent material candidate due to its significant spin-orbit coupling (SOC) and electrically-tunable properties. A key effect of an applied electric field is that it can either open or close the energy band gap, which is an important requirement for digital electronics applications. A variety of fascinating features of silicene have been discussed from a theoretical point of view. These include the quantum spin Hall and anomalous Hall effect, as well as valley-polarized quantum Hall effect under an electric field, anomalous Hall insulators and single-valley semimetals, potential giant magneto-resistance, and topologically protected helical edge states. [14–16] Germanene, on the other hand, is believed to acquire a much larger intrinsic spin-orbit gap 24-93 meV [17, 18], and only very few groups have managed to synthesize germanene [19–22] on different substrates.

A careful theoretical treatment of electron correlations in the materials under investigation is necessary since a qualitative difference between the results may be obtained from the employment of specific methods for calculations. The method we have used might be considered as a starting point for further analysis and may trigger higher level approximations in future works. Analytical calculation of the correlation energy requires a screened Coulomb interaction within the random-phase approximation (RPA). Earlier calculations of exchange and correlation energies have been reported for conventional 2D and 3D electron gases. [23, 24] It was pointed out by Barlas [25, 26] that both charge and spin susceptibilities in graphene are significantly reduced due to electron chirality, and this reduction is further enhanced at lower electron densities. Therefore, for silicene it is very interesting to see how the exchange and correlation energies are modified in the presence of a gap but the absence of electron chirality at the same time.

The low-energy model Hamiltonian for a puckered honeycomb lattice could be written as

$$\mathcal{H}_\xi = \hbar v_F (\xi k_x \hat{\tau}_x + k_y \hat{\tau}_y) - \xi \Delta_{\text{SO}} \hat{\sigma}_z \hat{\tau}_z + \Delta_z \hat{\tau}_z . \quad (1)$$

Here, the first term is the graphene Hamiltonian with  $v_F = 5 \times 10^5$  m/s,  $\hat{\tau}_{x,y,z}$  and  $\hat{\sigma}_{x,y,z}$  are Pauli matrices corresponding to two sub-spaces,  $\xi = \pm 1$  for  $K$  and  $K'$  points. The second term describes a Kane-Mele system [27] with a spin-orbit gap  $\Delta_{\text{SO}}$ . The last term represents the sublattice potential difference with  $\Delta_z = E_z d$  due to a perpendicular electric field  $E_z$ , where  $d \simeq 0.46 \text{ \AA}$  is the out-of-plane sublattice displacement due to buckling.

The Hamiltonian in Eq. (1) yields the low-energy dispersion relations

$$sE_k = \pm \sqrt{(\hbar v_F)^2 k^2 + \Delta_{\sigma,\xi}^2} , \quad (2)$$

where  $sE_k$  is the energy dispersion with  $s = 1$  ( $s = -1$ ) for the conduction (valence) band,  $\Delta_{\sigma,\xi} = |\sigma\xi\Delta_{\text{SO}} - \Delta_z|$  with  $\sigma = \pm 1$  represents two spin-resolved energy bandgaps, determined by either the sum or the difference between two gaps for two spin states (only electrons near the  $K$  point with  $\xi = 1$  are considered). Therefore, we can write  $\Delta_{>} = \Delta_{\text{SO}} + \Delta_z$  and  $\Delta_{<} = |\Delta_{\text{SO}} - \Delta_z|$ . A similar model Hamiltonian may be used to describe BP near the  $\Gamma$  and  $\Gamma'$  points.

When  $E_z = 0$ , the asymmetry gap  $\Delta_z = 0$  and the system behaves as a  $Z_2$  topological insulator (TI) or spin-Hall insulator due to the fact that two edge states in a silicene nanoribbon become gapless [12, 28] and  $\Delta_{<} = \Delta_{>} = \Delta_{\text{SO}}$ .

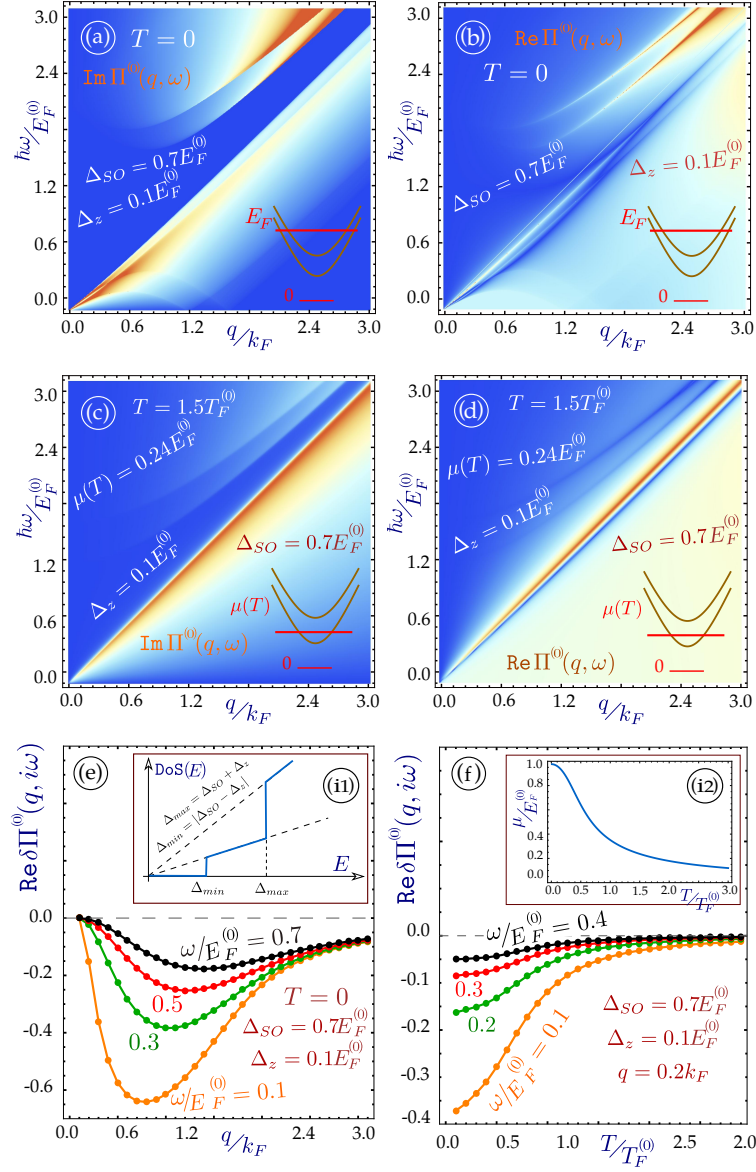


FIG. 1. (Color online) Panels (a) and (b) present density plots of the imaginary and real parts of the non-interacting polarizability  $\Pi^{(0)}(q, \omega)$  at  $T = 0$  as functions of frequency in units of  $\mu(T = 0) = E_F^{(0)}$  for  $\Delta_{SO} = 0.7E_F^{(0)}$  and  $\Delta_z = 0.1E_F^{(0)}$  (both spin-dependent subbands are doped and have energy gaps). Plots (c) and (d) show similar results at  $T = T_F^{(0)} \equiv E_F^{(0)}/k_B$ . Panel (e) displays the real part of the shifted polarizability  $\delta\Pi^{(0)}(q, i\omega)$  due to doping, as defined in Eq. (5), as a function of  $q$  at  $T = 0$  for various  $i\omega$  values, while plot (f) exhibits the real part of  $\delta\Pi^{(0)}(q, \omega)$  as a function of  $T$  for  $q = 0.2k_F$  ( $k_F = E_F^{(0)}/\hbar v_F$ ) and various  $i\omega$  values. All the results are scaled by the graphene density of states  $\text{DoS}(E_F^{(0)}) = 2E_F^{(0)}/\pi\hbar^2 v_F^2$  at the Fermi energy. Inset (i1) presents  $\text{DoS}(E)$  of silicene, while inset (i2) corresponds to  $\mu(T)$  of doped silicene.

Once  $E_z > 0$ , the minimal gap  $\Delta_{<}$  falls off linearly to zero, approaching a gapless conducting state. In this situation, only one energy gap, corresponding to a specific pair of subbands with  $\sigma = 1$  is closed. Such a state is referred to as a *valley-spin polarized metal* (VSPM). If  $E_z$  is further increased beyond this point, the system transfers to a trivial band insulator (BI) with no gapless edge states even far away from the  $K$ -points, and the energy gap keeps growing and never closes again.

The dynamical polarization function  $\Pi^{(0)}(q, \omega)$  is one of the most important quantities to determine the transport, collective and charge screening properties of a material. In the one-loop approximation, for a clean sample without impurity and phonon scatterings at low temperatures, is given by

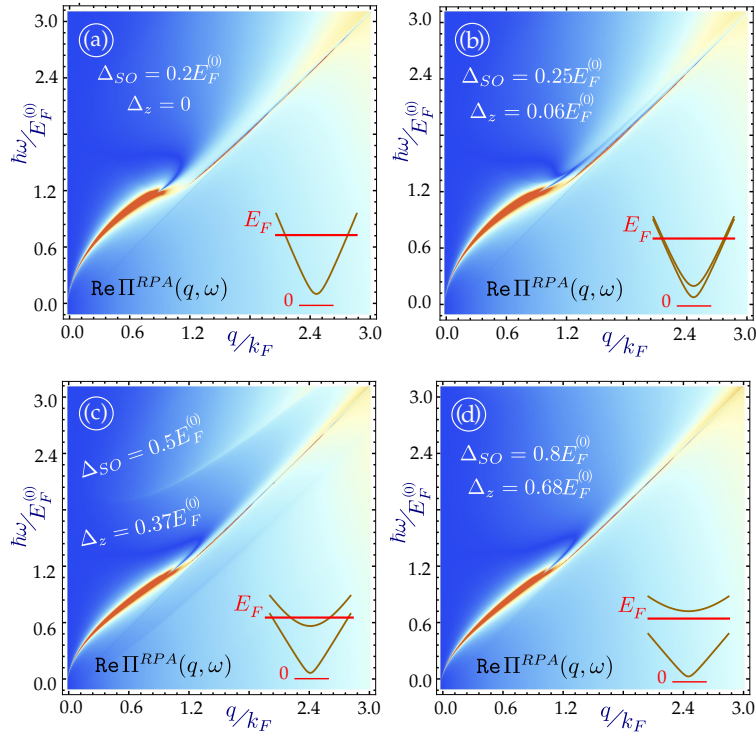


FIG. 2. (Color online) Split plasmon branches (peaks of the RPA polarization function) for different combinations of energy gaps  $\Delta_{SO}$  and  $\Delta_z$  in panels (a), (b) and (c). Panel (d) corresponds to the case with an unfilled upper subband.

$$\Pi^{(0)}(q, \omega) = \frac{1}{8\pi^2} \sum_{\sigma, \xi = \pm 1} \int d^2\mathbf{k} \sum_{s, s' = \pm 1} \left\{ 1 + ss' \frac{\hbar^2 v_F^2 (\mathbf{k} + \mathbf{q}) \cdot \mathbf{k} + \Delta_{\sigma, \xi}^2}{E_k E_{|\mathbf{k} + \mathbf{q}|}} \right\} \frac{f_0(sE_k - \mu, T) - f_0(s'E_{|\mathbf{k} + \mathbf{q}|} - \mu, T)}{sE_k - s'E_{|\mathbf{k} + \mathbf{q}|} - \hbar(\omega + i0^+)}, \quad (3)$$

where  $f_0(sE_k - \mu, T)$  is the Fermi-Dirac distribution function for a given subband,  $\mu$  and  $T$  are the chemical potential and temperature of the system. Equation (3) is just an average of two graphene polarizabilities with two inequivalent energy gaps  $\Delta_<$  and  $\Delta_>$ , i.e., two subband pairs contribute equivalently. Such a fact is often used in describing many-body properties of silicene. [11] The imaginary part of  $\Pi^{(0)}(q, \omega)$ , presented in Fig.1 (a) and (c) shows the single-particle excitation regions or the particle-hole modes (PHM's), i.e., those regions where a plasmon is Landau damped by breaking it into electron-hole excitations.

Plasmons are obtained from zero of the dielectric function given by  $\epsilon^{(0)}(q, \omega) = 1 - V(q) \Pi^{(0)}(q, \omega)$ , where  $V(q) = e^2/2\epsilon_0\epsilon_b q$  is the two-dimensional Coulomb interaction and  $\epsilon_b$  is the dielectric constant of the host material. Examples of plasmons in silicene are shown in Fig.2 and will be discussed below.

The central subject of the current study is the  $T$  dependence of the many-body effects in silicene. It is known that  $\mu$  decreases with  $T$  for fixed doping level. The existence of an infinite sea of holes below the Dirac points guarantees  $\mu > 0$  and  $\mu \rightarrow 0$  in the high- $T$  limit. In order to obtain the result for silicene, we have to calculate the density of states. Our early study [29] revealed that the density of states of graphene is not changed in the presence of an energy bandgap for the energies above the gap. This should also be valid for silicene with the two pairs of subbands separated by energy gaps. The calculated density of states  $\text{DoS}(E)$  is a piece-wise linear function, which is presented in the inset (i1) of Fig.1, and the chemical potential  $\mu(T)$  for silicene, quite similar to graphene, is shown in another inset (i2).

Although plasmon excitations in silicene have attracted some attentions recently, [11, 30, 31] there is an interesting experimental observation which is still lack of a clear explanation. For a graphene with an energy gap in the range of  $\Delta_0 \simeq (0.20 - 0.22)\mu$ , the plasmon mode was found first to enter into and then exit from the particle-hole continuum, leading to *split or "broken"* undamped plasmon branch. [32] Such an extended undamped plasmon mode is of key interest to a number of applications, such as plasmonic metamaterials, nanoarrays and tunable hybrid optical devices. [33] For silicene, we have found this split plasmon occurs within a compensated spin-orbit gap  $\Delta_{SO}$  by a

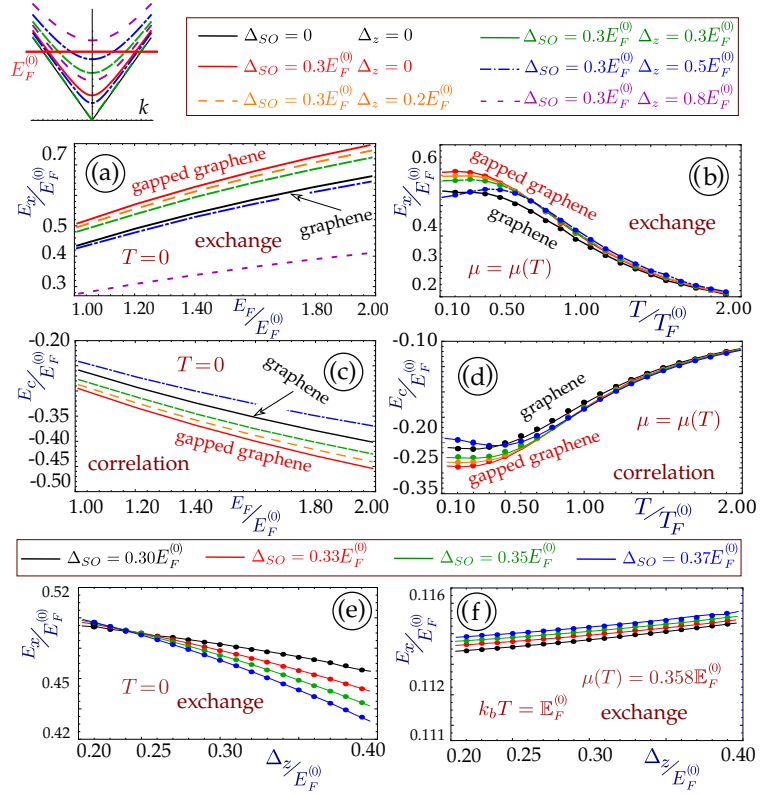


FIG. 3. (Color online) Exchange ( $E_x$ ) and correlation ( $E_c$ ) energies for graphene and silicene with different energy gaps at various  $T$ . Plots (a) and (c) demonstrate doping dependence of  $E_x$  and  $E_c$  at  $T = 0$  for graphene (black solid curve), gapped graphene or silicene with  $\Delta_z = 0$  (red solid curve) and for different combinations of  $\Delta_{SO}$  and  $\Delta_z$ . Panels (b) and (d) show the  $T$  dependence of  $E_x$  and  $E_c$  with fixed doping ( $E_F \equiv \mu(T = 0) = E_F^{(0)}$ ). Plots (e) ( $T = 0$ ) and (f) ( $T = E_F/k_B$ ) display the  $\Delta_z$  dependence of silicene  $E_x$  with different  $\Delta_{SO}$  to demonstrate the TI $\rightarrow$ VSPM $\rightarrow$ BI phase transition.

field-induced one  $\Delta_z$ . Our numerical results for a split plasmon branch with various combinations of these two gaps are shown in Fig. 2. The minimum gap  $\Delta_<$  determines the outermost boundary of the PHM region and gives rise to a PHM-free region for the plasmon branch at finite wave vector  $q$ . In general, each of two gaps affects the behavior of the plasmon branch independently. If both spin-split subbands are occupied as  $\mu > \Delta_>$ , the plasmon frequency in the long-wavelength limit becomes  $\simeq \sqrt{(\mu^2 - \Delta_{SO}^2 - \Delta_z^2)} q$ . In this case, both gaps play the same role by reducing the plasmon frequency. Although we cannot derive an analytic expression for the plasmon dispersion relation at large  $q$  values, the general feature from our numerical results in Fig. 2 may be summarized as follows: both  $\Delta_{SO}$  and  $\Delta_z$  reduce the plasmon frequency, causing the plasmon branch to stay closer to the main diagonal. We further note that the split plasmon branch survives even for the case with only one occupied subband, as shown in Fig. 2(d). Here, all our calculations for the plasmon dispersion relation were conducted at  $T = 0$ .

We now turn our attention to calculating the exchange and correlation energies of silicene. For convenience, we omit the theoretical derivation but simply write down expressions used in our calculations, based on the *interaction energy* integral [34] for the jellium model as well as the fluctuation-dissipation-theorem. [25, 35] Within this model, the calculated energy appears to be divergent. This divergence, however, can be removed, if we consider only doped electrons above the Dirac point, i.e. choosing the total energy of intrinsic graphene as the zero-energy point. [25, 36]. We also apply an upper limit  $Q_c$  for the  $q$ -integral since the Dirac-cone approximation for silicene is valid only up to 0.46 eV. The calculated exchange energy is

$$E_x = -\frac{\hbar}{2\pi n} \int_0^{Q_c} \frac{d^2 \mathbf{q}}{(2\pi)^2} V(q) \int_0^\infty d\omega \delta\Pi^{(0)}(q, i\omega), \quad (4)$$

where the shifted polarizability related to doping is

$$\delta\Pi^{(0)}(q, i\omega) = \Pi^{(0)}(q, i\omega; \mu) - \Pi^{(0)}(q, i\omega; \mu = 0). \quad (5)$$

At  $T = 0$ , the doping contribution to the polarization function could be easily separated [32] since the Fermi-Dirac distribution is just a unit-step function. The correlation energy is now given in the RPA by

$$E_c = -E_x + \frac{\hbar}{2\pi n} \int_0^{Q_c} \frac{d^2\mathbf{q}}{(2\pi)^2} \int_0^\infty d\omega \ln \left[ \frac{1 - V(q) \Pi^{(0)}(q, i\omega; \mu)}{1 - V(q) \Pi^{(0)}(q, i\omega; 0)} \right]. \quad (6)$$

Our numerical results for the exchange-correlation energy are presented in Fig. 3. If silicene is undoped at  $T = 0$ ,  $\mu(T) = 0$  is maintained for all  $T$ , which yields a common reference point. Results for  $\delta\Pi^{(0)}(q, i\omega)$  with doping as functions of  $q$  and  $T$  are displayed in Fig. 1[(e),(f)]. At  $T = 0$ , the doping effect is only limited to a region covered by small values of  $q$  and  $\omega$ . In addition,  $\delta\Pi^{(0)}(q, i\omega)$  decreases with increasing  $T$ . Such behaviors are expected by noticing very small  $\text{Re}[\Pi^{(0)}(q, i\omega)]$  for the interband transitions above the main diagonal as shown in Figs. 2[(b),(c)]. We also find that  $E_x$  and  $E_c$ , except for being opposite to each other, behave similarly in various situations. This implies that the log-term in Eq. (6) is finite but insignificant to the correlation. At  $T = 0$ ,  $E_x$  in Fig. 3(a) increases with doping since more electrons may contribute. Interestingly, even the exchange-correlation energy per electron also increases with the doping, as shown in Fig. 3[(a),(c)], due to enhanced many-body effects. Moreover, from Fig. 3(e), we find that the exchange energy is increased for a larger energy gap, which agrees with earlier reported results in Ref. [36]. Therefore, we may state that  $E_x$  and  $|E_c|$  for silicene will increase with  $\Delta_<$ . On the other hand,  $E_x$  decreases as  $T$  is increased, similar to  $\mu(T)$ . Quantitatively, crossing of curves for different combinations of  $\Delta_{\text{SO}}$  and  $\Delta_z$  are found in Fig. 3[(b),(d)]. Results for the  $\Delta_z$  dependence of the exchange energy on  $\Delta_z$  are compared in Fig. 3[(e),(f)] at zero and a finite temperature, where different points for the TI $\rightarrow$ VSPM $\rightarrow$ BI transition are found by varying  $\Delta_{\text{SO}}$ .

In summary, we have obtained extensive numerical results for the exchange and correlation energies in silicene at various temperatures and energy gaps and found that they increase with doping but decrease with temperature. The  $\Delta_z$  dependence of exchange energy with various  $\Delta_{\text{SO}}$  changes significantly as  $T$  increases.

In contrast to gapped graphene, for plasmon excitations in silicene, we have demonstrated the breaking down of a single plasmon branch into two undamped pieces, appearing for different combinations of  $\Delta_{\text{SO}}$  and  $\Delta_z$ . Some of these combinations correspond to one unoccupied subband with  $\mu < \Delta_>$ .

Since silicene, germanine and other puckered lattices are believed to be promising replacements for graphene and topological insulators, we expect that extensive knowledge on plasmonic properties of these materials, such as exchange and correlation corrections to the electron kinetic energy, local compressibility and susceptibility, become crucial for applying to fabrication of semiconductor electronic devices, developing spintronics and many other new areas of interests.

- 
- [1] K. Novoselov, A. K. Geim, S. Morozov, D. Jiang, M. Katsnelson, I. Grigorieva, S. Dubonos, and A. Firsov, *nature* **438**, 197 (2005).
- [2] A. K. Geim and K. S. Novoselov, *Nature materials* **6**, 183 (2007).
- [3] A. C. Neto, F. Guinea, N. Peres, K. S. Novoselov, and A. K. Geim, *Reviews of modern physics* **81**, 109 (2009).
- [4] H.-R. Chang, J. Zhou, H. Zhang, and Y. Yao, *Phys. Rev. B* **89**, 201411 (2014).
- [5] G. Giovannetti, P. A. Khomyakov, G. Brocks, P. J. Kelly, and J. van den Brink, *Physical Review B* **76**, 073103 (2007).
- [6] N. Kharche and S. K. Nayak, *Nano letters* **11**, 5274 (2011).
- [7] Z. H. Ni, T. Yu, Y. H. Lu, Y. Y. Wang, Y. P. Feng, and Z. X. Shen, *ACS nano* **2**, 2301 (2008).
- [8] O. Kibis, *Physical Review B* **81**, 165433 (2010).
- [9] A. N. Rudenko and M. I. Katsnelson, *Phys. Rev. B* **89**, 201408 (2014).
- [10] Q. Liu, X. Zhang, L. B. Abdalla, A. Fazio, and A. Zunger, *Nano Letters* **15**, 1222 (2015).
- [11] C. J. Tabert and E. J. Nicol, *Phys. Rev. B* **89**, 195410 (2014).
- [12] M. Ezawa, *New Journal of Physics* **14**, 033003 (2012).
- [13] M. Ezawa, *Phys. Rev. Lett.* **109**, 055502 (2012).
- [14] B. Aufray, A. Kara, S. Vizzini, H. Oughaddou, C. Leandri, B. Ealet, and G. Le Lay, *Applied Physics Letters* **96**, 183102 (2010).
- [15] P. De Padova, C. Quaresima, C. Ottaviani, P. M. Sheverdyaeva, P. Moras, C. Carbone, D. Topwal, B. Olivieri, A. Kara, H. Oughaddou, *et al.*, *Applied Physics Letters* **96**, 261905 (2010).
- [16] B. Lalmi, H. Oughaddou, H. Enriquez, A. Kara, S. Vizzini, B. Ealet, and B. Aufray, *Applied Physics Letters* **97**, 223109 (2010).

- [17] L. Zhang, P. Bampoulis, A. van Houselt, and H. Zandvliet, *Applied Physics Letters* **107**, 111605 (2015).
- [18] A. Acun, L. Zhang, P. Bampoulis, M. Farmanbar, A. van Houselt, A. Rudenko, M. Lingenfelder, G. Brocks, B. Poelsema, M. Katsnelson, *et al.*, *Journal of Physics: Condensed Matter* **27**, 443002 (2015).
- [19] L. Li, S.-z. Lu, J. Pan, Z. Qin, Y.-q. Wang, Y. Wang, G.-y. Cao, S. Du, and H.-J. Gao, *Advanced Materials* **26**, 4820 (2014).
- [20] M. Dávila, L. Xian, S. Cahangirov, A. Rubio, and G. Le Lay, *New Journal of Physics* **16**, 095002 (2014).
- [21] P. Bampoulis, L. Zhang, A. Safaei, R. Van Gastel, B. Poelsema, and H. J. W. Zandvliet, *Journal of physics: Condensed matter* **26**, 442001 (2014).
- [22] M. Derivaz, D. Dentel, R. Stephan, M.-C. Hanf, A. Mehdaoui, P. Sonnet, and C. Pirri, *Nano letters* **15**, 2510 (2015).
- [23] J. Harris and R. Jones, *Journal of Physics F: Metal Physics* **4**, 1170 (1974).
- [24] A. Griffin, J. Harris, and H. Kranz, *Journal of Physics F: Metal Physics* **4**, 1744 (1974).
- [25] Y. Barlas, T. Pereg-Barnea, M. Polini, R. Asgari, and A. MacDonald, *Physical review letters* **98**, 236601 (2007).
- [26] M. Polini, R. Asgari, Y. Barlas, T. Pereg-Barnea, and A. H. MacDonald, *Solid State Communications* **143**, 58 (2007).
- [27] C. L. Kane and E. J. Mele, *Phys. Rev. Lett.* **95**, 226801 (2005).
- [28] C.-C. Liu, W. Feng, and Y. Yao, *Phys. Rev. Lett.* **107**, 076802 (2011).
- [29] A. Iurov, G. Gumbs, D. Huang, and V. Silkin, *Physical Review B* **93**, 035404 (2016).
- [30] H.-R. Chang, J. Zhou, H. Zhang, and Y. Yao, *Physical Review B* **89**, 201411 (2014).
- [31] J. Wu, S. Chen, and M. Lin, *New Journal of Physics* **16**, 125002 (2014).
- [32] P. Pyatkovskiy, *Journal of Physics: Condensed Matter* **21**, 025506 (2008).
- [33] A. Politano and G. Chiarello, *Nanoscale* **6**, 10927 (2014).
- [34] G. Gumbs and D. Huang, *Properties of Interacting Low-Dimensional Systems* (John Wiley & Sons, 2013).
- [35] G. Giuliani and G. Vignale, *Quantum theory of the electron liquid* (Cambridge university press, 2005).
- [36] A. Qaiumzadeh and R. Asgari, *Physical Review B* **79**, 075414 (2009).